ISSN 1063-7761, Journal of Experimental and Theoretical Physics, 2020, Vol. 130, No. 1, pp. 69–75. © Pleiades Publishing, Inc., 2020.
Russian Text © The Author(s), 2020, published in Zhurnal Eksperimental'noi i Teoreticheskoi Fiziki, 2020, Vol. 157, No. 1, pp. 82–89.

SOLIDS AND LIQUIDS

Phonon Spectrum and Structural Transformations at High Pressures in Vanadyl IV Phthalocyanine Crystals

K. P. Meletov[a,*], A. V. Kuzmin[a], and R. P. Shibaeva[a]

[a] *Institute of Solid State Physics, Russian Academy of Sciences, Chernogolovka, Moscow oblast, 142432 Russia*

**e-mail: mele@issp.ac.ru*

Received May 27, 2019; revised June 28, 2019; accepted July 1, 2019

Abstract—The Raman scattering spectra and crystalline structure of vanadyl IV phthalocyanine (VOPc) at normal and high pressures has been studied. According to the X-ray diffraction data, the initial microcrystalline powder represented a mixture of the triclinic α phase (79%) and the monoclinic β phase (21%) possessing $P\bar{1}$ and $P2_1/c$ symmetry, respectively. Raman spectra of the two phases are similar, but the phonon modes of the β phase are shifted toward higher frequencies (energies). The pressure dependence of the spectra of the α phase has been determined and it is established that the interval of 2.3–3.4 GPa reveals reversible pressure-dependent variations: above 3 GPa, some phonon modes exhibit splitting and the coefficients of pressure-induced (baric) shift for almost all modes show a decrease. A high-pressure feature observed in the Raman spectra can be related to changes in intermolecular interactions in crystalline structure of the α phase. The pressure dependence of the α phase unit cell volume measured at pressures increasing up to 4 GPa is a smooth monotonic function that can be well described by the Murnaghan equation of state. The obtained data were used to calculate the Grüneisen parameters of VOPc phonon modes.

DOI: 10.1134/S1063776119110141

1. INTRODUCTION

Phthalocyanine (Pc) is a planar π-conjugated macrocyclic molecule representing a heterocycle comprising 8 nitrogen atoms and 32 carbon atoms, the center of which can accommodate coordinated ligand M or $M^{IV}O$, where M is a tetravalent metal atom (to yield chemical formula $C_{32}H_{16}N_8M^{IV}O$). High stability of the Pc structure accounts for its wide use in various fields of science, technology, and medicine including nonlinear optics, photovoltaics and new materials for solar cells, liquid crystals, dyes, and contrast agents for magnetic-resonance tomography [1–4]. The optical properties, phonon spectrum, and structure of neutral metal phthalocyanines have been rather well studied in numerous experiment and numerical calculations [5–7]. Polymorphous transformations in thin metal-free H_2Pc films on annealing were studied by X-ray diffraction (XRD) and resonance Raman scattering spectroscopy for elucidating the mechanism of transitions from α to β phase [8–10]. The structure and phonon spectra of negatively charged (reduced) metal phthalocyanine were numerically calculated with and without allowance for the Jahn–Teller (JT) distortions [11].

In recent years, much effort has been devoted to the synthesis of new materials based on the reduced forms of phthalocyanines representing molecular donor–acceptor complexes. These complexes have involved layered structures in which metal phthalocyanine layers are alternating with donor layers consisting of various organic molecules [12–15]. Considerable interest in these complexes is related to their ability of possessing promising magnetic properties and metallic conductivity caused by the delocalization of electrons passing from the donor molecules to macrocycles [16, 17]. The electric conductivity of acceptor at high pressures (against dielectric properties at normal pressure) was studied long ago [18, 19] and it was established that the resistivity exhibited significant (about eight orders of magnitude) decrease as the pressure increased up to about 30 GPa.

As is known, the excess charge on a macrocycle leads to significant changes in the phonon spectrum of metal phthalocyanines [20], so that phthalocyanine complexes with charge transfer or $[M^{IV}OPc]$ anion-based complexes are worth of special attention. During the reduction of $[M^{IV}OPc]$, degenerate levels are populated with additional electrons "triggering" first-order JT interaction, so that the Pc macrocycle is deformed, degeneracy is removed, and JT-anion $[M^{IV}OPc]^{n-}$ is formed.

Metal phthalocyanines in the crystalline form represent molecular crystals featuring weak van der Waals interactions. For this reason, the phonon spectra and crystalline structure of metal phthalocyanines are very sensitive to decrease in intermolecular distances, in

particular, distances between macrocycles of neighboring molecules. Studying the intermolecular interactions of acceptor phthalocyanine at high pressures can provide important information for optimization of the synthesis of donor–acceptor complexes.

The present work was aimed at studying the behavior of vanadyl IV phthalocyanine (VOPc) microcrystals at high pressures by Raman spectroscopy and XRD techniques. The samples were prepared as microcrystalline powders comprising a mixture of triclinic α phase (79%) and monoclinic β phase (21%) possessing $P\bar{1}$ and $P2_1/c$ symmetry, respectively. Raman spectra of both α and β phases were measured and proved to be almost identical, but the phonon modes of β phase had somewhat higher frequencies. The spectra of α phase were measured at various pressures up to 10 GPa and the baric dependence of phonon modes was determined. It is established that the pressure interval of 2.3–3.4 GPa has a reversible pressure-dependent feature that is related to the splitting of some high-frequency modes and a decrease in the coefficients of baric shift of almost all modes. The XRD measurements on VOPc powders at high pressures were performed and the baric dependence of the α phase unit cell volume was determined up to 4 GPa. This dependence is a smooth monotonic function of the pressure that can be well described by the Murnaghan equation of state:

$$\left(\frac{V_0}{V}\right)^{B'} = 1 + P\frac{B'}{B_0}, \quad (1)$$

where $B_0 = 8.5 \pm 0.9$ GPa is the bulk modulus and $B' = \partial B_0/\partial P = 5.6 \pm 0.6$. It is shown that a peculiarity in the baric dependence of phonon modes is probably related to the formation of a hydrogen bond (H-bond) between oxygen atom of the VOPc molecule and peripheral H atom of the C–H bond of isoindole ring of the neighboring molecule. The obtained Raman spectroscopy and XRD data were used to calculate the Grüneisen parameters of VOPc phonon modes.

2. EXPERIMENT

All measurements were performed on microcrystalline VOPc samples isolated from a commercially available powder (Acros Organics). Raman spectra were obtained for a selected sample with characteristic size about 60 μm and good surface quality. These measurements were performed in backscattering geometry on a setup comprising Acton SpectraPro-2500i equipped with Pixis2K CCD detector cooled to –70°C and Olympus microscope. The sample response was excited by a diode-pumped continuous-wave solid-state laser (λ = 532 nm). The laser beam was focused on the sample with the aid of an Olympus 50× objective to a spot with diameter about 1.3 μm. Spurious laser emission line in the scattered beam was suppressed using an edge filter (532 μm) with an optical density of 6 and passband from +140 cm^{-1}. The incident laser beam intensity immediately in front of diamond anvil cell was about 250 μW. Raman scattering measurements at high pressures were performed in a chamber with diamond anvils of the Mao–Bell type. Primary XRD analysis and qualitative identification of the initial powder structure at normal pressure were performed on Siemens D-500 powder diffractometer using CuK_α radiation. The XRD measurements on powders at high pressures were carried out on Oxford Diffraction Gemini R diffractometer using MoK_α radiation, equipped with two-coordinate cooled CCD detector. The XRD experiments at high pressures were performed with VOPc powder in a chamber with diamond anvils of the Boehler type. The pressure transmitting medium was a 4 : 1 (v/v) mixture of methyl and ethyl alcohols, and the pressure magnitude was calibrated using spectral position of the R_1 luminescence line of a ruby crystal [21]. The XRD patterns were computer processed and integrated using CrysAlisPro software system [22] and the full-profile analysis was carried out in Profex user interface [23].

3. RESULTS AND DISCUSSION

Figure 1 (bottom curve) shows the XRD pattern measured under normal pressure for the initial VOPc powder. Qualitative phase analysis of the experimental diffractogram established that the initial sample represented a mixture of triclinic (α) and monoclinic (β) phases. The structure of single crystals of the α phase was described in [24, 25]. A comparison of the unit cell parameters determined for VOPc crystals studied in the present work to the corresponding values for α and β phases of titanyl phthalocyanine (TiOPc) [26] shows that these VOPc and TiOPc crystals are isostructural. Exact data on the structures of single-crystalline triclinic and monoclinic phases of titanyl phthalocyanine were also presented in [26], which allowed us to take the atomic coordinates of monoclinic TiOPc phase as starting data for refinement of the structure of monoclinic VOPc phase by the Rietveld method. The unit cell parameters, positions, and orientations of VOPc molecules were refined relative to the crystallographic axes of α and β phases. In order to fix the shape of VOPc molecules, rigid limitations were imposed on the bond lengths, valence angles, and dihedral angles in the macrocycle of metal phthalocyanine.

Based on the results of XRD analysis, it was established that triclinic α phase is the dominating component (79%) in the initial VOPc powder, while monoclinic β phase accounts for about 21%. Theoretical XRD patterns calculated using refined structural data for the two phases are presented in the middle and top parts of Fig. 1, while the refined structural parameters and full-profile fitting results are listed in Table 1. The right-hand panel in Fig. 1 shows the mutual arrange-

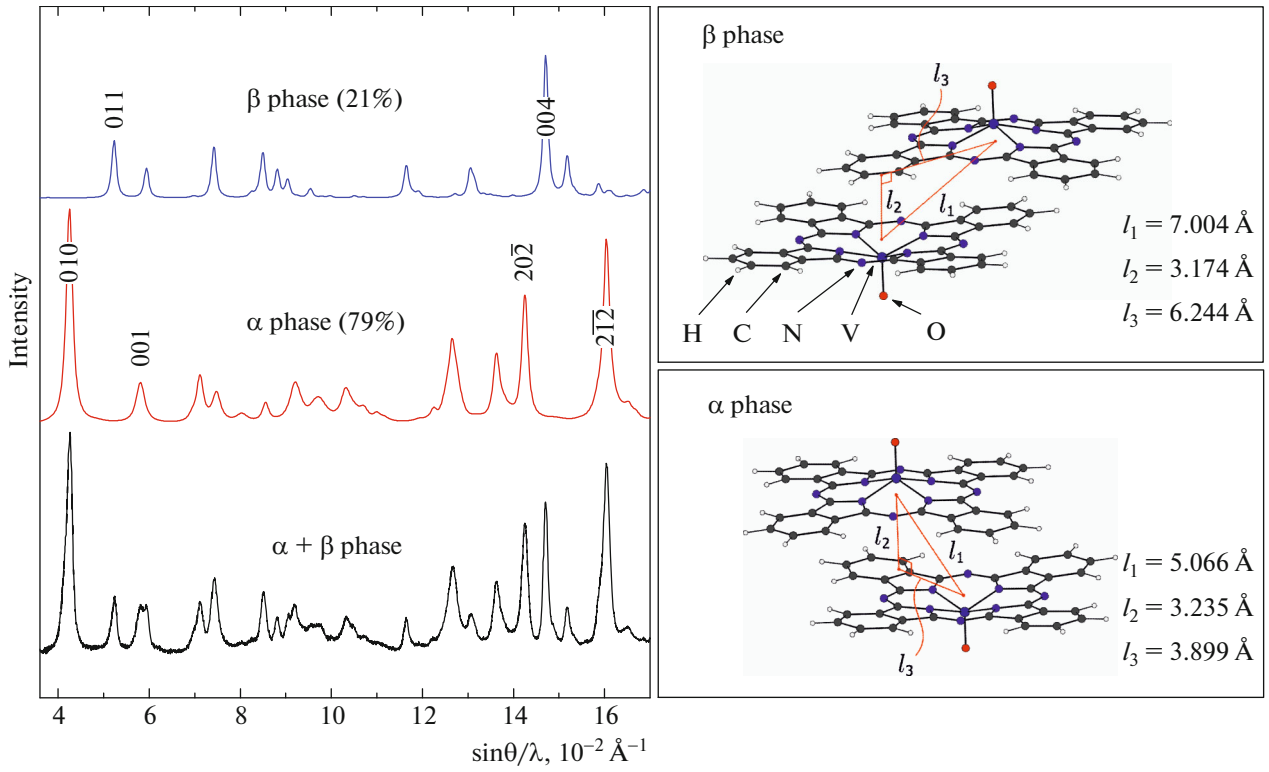

Fig. 1. (Color online) XRD patterns of vanadyl IV phthalocyanine powder under normal conditions: bottom curve presents the measured diffractogram of the initial powder; middle and top curves show the results of qualitative phase analysis; right-hand panel shows the arrangement of molecules in the unit cells of α and β phases.

ment of nearest-neighbor VOPc molecules in the unit cell as determined as a result of structure optimization for the α and β phases. It should be noted that the planes of macrocycles in the β phase are situated closer to each other, so that the distance between these planes in the β phase (l_2 = 3.174 Å) is smaller than that (l_2 = 3.235 Å) in the α phase. This difference implies, in particular, that the van der Waals interaction between macrocycles of the neighboring molecules in the β phase is stronger than in the α phase, which can lead to increase in the frequencies of intramolecular phonon modes,

Indeed, the Raman spectra of VOPc microcrystals isolated from the initial powder in most selected samples had the form presented in Fig, 2 (lower curve). In some rare cases, phonon bands in the Raman spectra of selected crystallites were somewhat shifted toward higher frequencies (energies) although the general structure of spectra was almost identical (Fig. 2, upper curve). Since the major fraction (79%) of crystallites belonged to the α phase, the lower spectrum in Fig. 2 should most probably be attributed to this phase. The frequencies of phonon modes in the upper spectrum of Fig. 2 (supposedly, β phase) are higher than those of the same modes in the lower spectrum, the difference reaching up to 10 cm^{-1}. This is related to decreased distances and enhanced interaction between macrocycles in the β phase.

The symmetry of VOPc molecule, as well as the molecules of other neutral metal phthalocyanines corresponds to point group C_{4v}. The total number of normal vibrational modes in this molecule is 58 × 3 – 6 =

Table 1. Structural parameters of the α and β phases of VOPc crystals.

	α-VOPc	β-VOPc
a, Å	12.195(1)	13.778(1)
b, Å	12.6500(5)	13.353(1)
c, Å	8.6202(4)	13.9898(3)
α	96.271(4)°	90°
β	95.382(5)°	103.614(4)°
γ	68.039(5)°	90°
V, Å^3	1323.97(1)	2501.6(2)
Z	2	4
Sp. group	$P\bar{1}$	$P2_1/c$

Refinement parameters: R = 6.38%; R_p = 4.57%; R_{wp} = 5.85%, R_{exp} = 0.97%; 5500 observable parameters; 1498 reflections; 59 refined parameters; angle (2θ) interval, 5°–60°; angle (2θ) step, 0.02°.

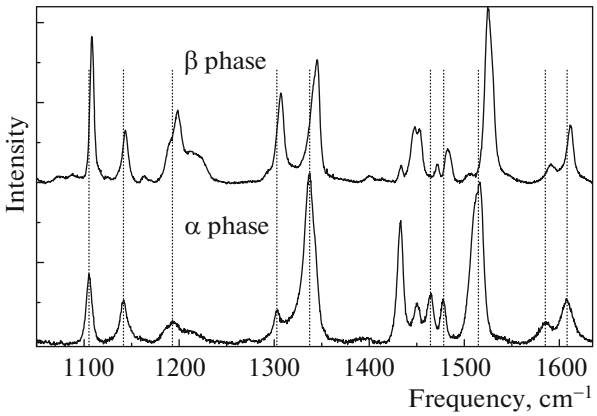

Fig. 2. Raman spectra of VOPc α and β phases measured in 1000–1700 cm^{-1} frequency range under normal conditions.

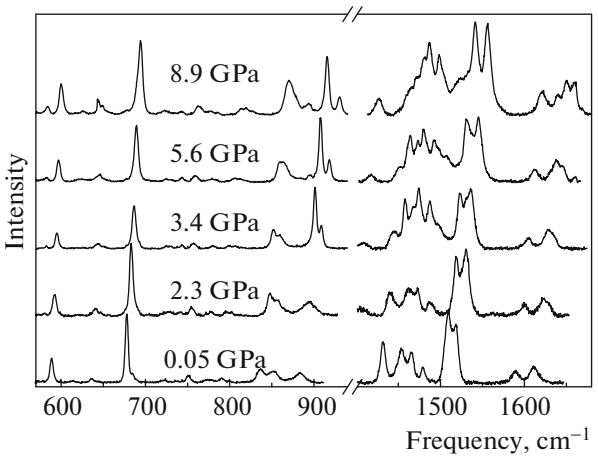

Fig. 3. Raman spectra of the VOPc α phase measured in 550–900 and 1450–1700 cm^{-1} frequency intervals at pressures increasing up to about 9 GPa.

168 and can be expanded into a sum of irreducible representations as $\Gamma_{vib} = 23A_1 + 19A_2 + 21B_1 + 21B_2 + 42E$. Since the crystal unit cell contains two molecules, the total number of vibrational modes is doubled and amounts to 348. In space group $P\bar{1}$, these vibrations can be expanded into a sum of irreducible representations as $\Gamma_{vib} = 174A_g + 174A_u$. The vibrations correspond to intermolecular and intramolecular phonon modes, those with lowest frequencies belonging to 12 intermolecular acoustical and optical modes related to the translational and rotational oscillations of rigid molecules in the lattice. The overwhelming majority of phonon modes in the crystal are intramolecular, related to atomic oscillations in the molecule [6]. The Raman spectra of VOPc were measured in a frequency range from 550 to 1680 cm^{-1} corresponding to the intramolecular phonon modes.

Figure 3 presents a series of Raman spectra of the VOPc α phase measured at high pressures up to about 10 GPa. These measurements were performed in cycles with both increasing and decreasing pressure (the reverse order of pressure variation is not presented in Fig. 3, where the frequency interval containing intense phonon mode from diamond anvils at about 1333.4 cm^{-1} is also rejected). As the pressure was increased, the frequencies of all phonon modes exhibited growth while the general structure of the spectrum remained unchanged up to a pressure of about 2.3 GPa. At a pressure of 3.4 GPa, some phonon modes in the Raman spectrum exhibited splitting. With further growth of the pressure, the extent of splitting increased while the rate of pressure-induced frequency shift for most modes decreased.

Figure 4 shows baric dependences of the VOPc phonon modes in a range of pressures up to 10 GPa for phonon frequencies in the (a) 595–925 and (b) 1430–1560 cm^{-1} intervals. As can be seen, these dependences are fully reversible with respect to pressure. In addition, these dependences exhibited peculiarities in the region of 2.3–3.4 GPa that could be related to the splitting of some phonon modes and a decrease in the coefficients of baric shift for almost all modes. The values of phonon frequencies at normal pressure and the coefficients of their baric shift at $P < 2.3$ GPa and $P > 3.4$ GPa are presented in the first, second, and third columns of Table 2. As can be seen from these data, the baric coefficients at $P > 3.4$ GPa decrease for all modes and the coefficient for 775.6 cm^{-1} mode even becomes negative. The phonon modes observed at 883.9, 1466, and 1479.5 cm^{-1} exhibit splitting, and the baric shift coefficient for one of the two components of 1479.5 cm^{-1} mode is increasing. The baric shift coefficients of VOPc are characteristic of intramolecular phonon modes and close to the well-known values for, e.g., classical molecular crystal of naphthalene [27]. This behavior is explained primarily by the fact that both these molecules contain isoindole rings, and a significant number of observed modes are related to the oscillations of carbon and hydrogen atoms.

Peculiarities of the baric dependences of VOPc phonon modes are probably caused by a structural phase transition in the region of pressures within 2.3–3.4. In order to understand whether the observed changes in Raman spectra of VOPc were caused by some changes in the crystalline structure, a series of XRD measurements were performed for the initial VOPc powder in the interval of pressures under consideration. Figure 5 shows powder diffractograms measured at various pressures up to 4.3 GPa and the obtained experimental plot of unit cell volume versus pressure.

The absence of peaks characteristic of the VOPc β phase in the XRD patterns measured at $P = 0.55$ GPa indicates that, already at rather low pressure, the residues of this phase in the initial powder mixture are

fully converted into the α phase. It should be noted that this transformation differs from the well-known transition from monoclinic ($C2/c$) α phase to monoclinic ($P2_1/a$) β phase in H_2Pc phthalocyanine during their annealing at high temperature [8]. The crystalline structure of VOPc powders does not change with further increase in the temperature and corresponds to a triclinic α phase. Results of the series of XRD measurements at various pressures allowed refinement of the parameters of crystalline lattice of the VOPc α phase and the position of Pc molecule in the unit cell. Figure 5b (open circles) shows the baric dependence of the unit cell volume, which is a smooth and monotonic function of pressure and can be adequately described by the Murnaghan equation of state (1).

The obtained value of bulk modulus B_0 is characteristic of molecular crystals and is related to their high compressibility, while a large value of B' is explained by rapid growth in the bulk modulus with increasing pressure. For the comparison, note that the bulk modulus of hardest mineral (diamond) is about 600 GPa, while the molecular crystal of naphthalene has $B_0 =$ 6.7 GPa and $B' = 7.1$ [28]. Using the obtained value of bulk modulus and data on the baric shift of bands in the Raman spectra, it is possible to calculate the values of Grüneisen parameters γ_i for the phonon modes of VOPc as

$$\gamma_i = \frac{\partial\Omega_i}{\Omega_i}\left(\frac{\partial V}{V}\right)^{-1} = \frac{B_0}{\Omega_i^0}\left(\frac{\partial\Omega_i}{\partial P}\right)^{-1}, \qquad (2)$$

where Ω_i^0 are the frequencies of phonon modes and $\partial\Omega_i/\partial P$ are the corresponding baric shift coefficients. The obtained values of Grüneisen parameters listed in the last column of Table 2 are typical of molecular crystals.

A comparative analysis of the refined atomic positions in VOPc structure at various pressures shows that deformation of the phthalocyanine sublattice during compression of the VOPc α phase is nonuniform. In particular, significant variations of relative shifts of the nearest neighbor macrocycles are observed at $P >$ 3 GPa. Figure 6 shows that this region of pressures features a jumplike displacement of the macrocycle of one Pc molecule relative to that of another molecule. The character of this displacement is illustrated in the right-hand inset to Fig. 6, which shows that it takes place in vertical direction in the figure plane and amounts to $v = 0.72$ Å. At this contraction, the lengths of short –H···O contacts between adjacent Pc molecules decrease, which can lead subsequently to the formation of H-bonds at higher pressures (Fig. 7). A closer packing of VOPc leads to a change in C–C–H pendulum vibrations in the isoindole rings whose peripheral H atoms are facing the axial oxygen of the nearest-neighbor molecule, while the frequencies of these vibrations in two other isoindole rings remain unchanged. The indicated changes lead to splitting of

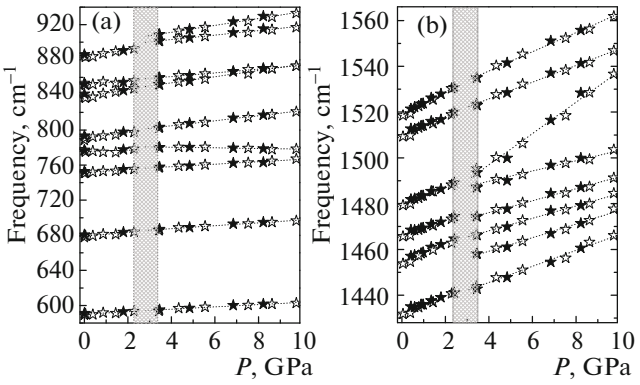

Fig. 4. Baric dependences of the VOPc phonon modes in (a) 580–920 and (b) 1450–1560 cm^{-1} frequency intervals. Bright and dark symbols refer to increasing and decreasing pressure, respectively, in the given cycle. Dashed curves show approximation of the experimental data by linear dependences in the regions of pressure below 2.3 GPa and above 3.4 GPa, respectively.

the corresponding intramolecular phonon modes observed in our Raman spectra of VOPc at high pressures [29]. A decrease in the baric shift coefficients of phonon modes observed at $P > 3$ GPa can also be related to the formation of additional H-bonds.

In concluding, we have studied the baric dependence of Raman spectra of the vanadyl IV phthalocyanine α phase and observed a reversible pressure-

Table 2. Calculated Grüneisen parameters of the VOPc α phase phonon modes

Ω_i^0, cm^{-1}	$\partial\Omega_i/\partial P$, cm^{-1}/GPa		γ_i
	$P < 2.3$ GPa	$P > 3.4$ GPa	
590	1.4	1.3	0.0115
679.1	2.1	1.6	0.0067
751.7	1.7	1.4	0.0074
775.6	0.6	−0.4	0.0204
790.8	3.1	2.9	0.0039
837.9	4.0	3.5	0.0028
852.3	1.5	2.1	0.0074
883.9	3.8	2.6	0.0028
883.9	3.8	3.9	0.0028
1432.2	3.8	3.5	0.0018
1454.3	4.2	3.0	0.0016
1466	3.4	2.7	0.0019
1466	3.4	2.6	0.0019
1479.5	4.0	2.3	0.0016
1479.5	4.0	6.8	0.0016
1509.7	4.2	3.8	0.0015
1518.6	5.1	4.2	0.0012

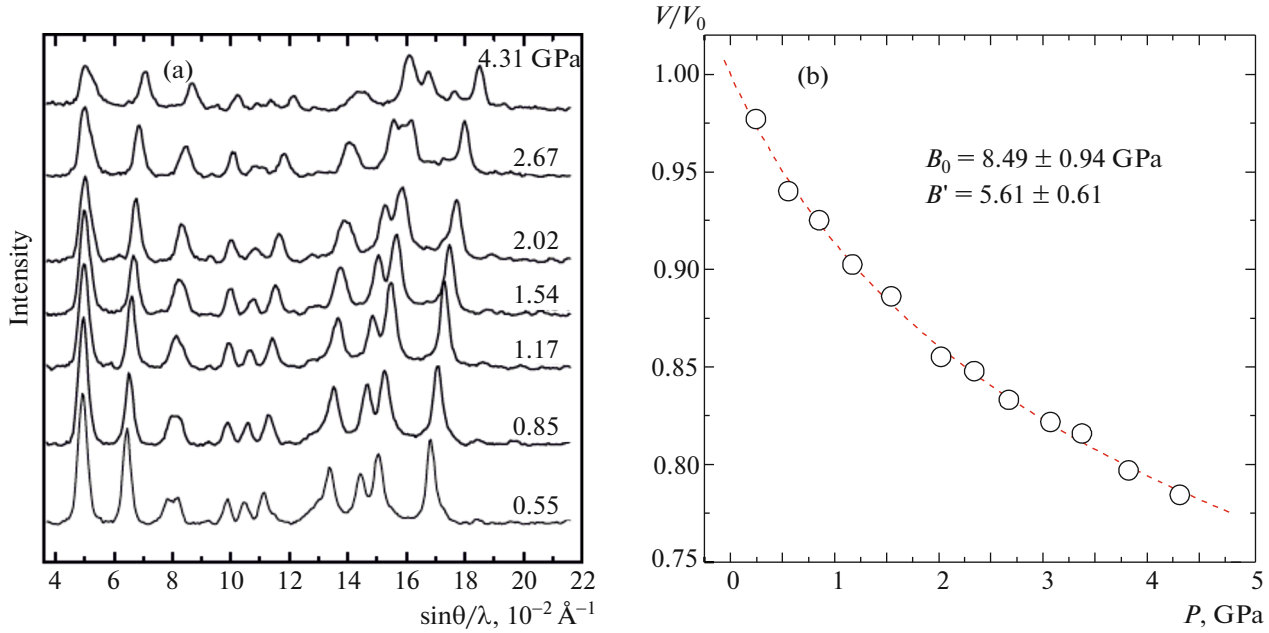

Fig. 5. (Color online) (a) XRD patterns of vanadyl IV phthalocyanine α phase measured at various pressures up to 4.2 GPa. (b) Pressure dependence of the relative unit cell volume: open circles represent experimental data, dashed curve shows an approximation according to the Murnaghan equation of state (1).

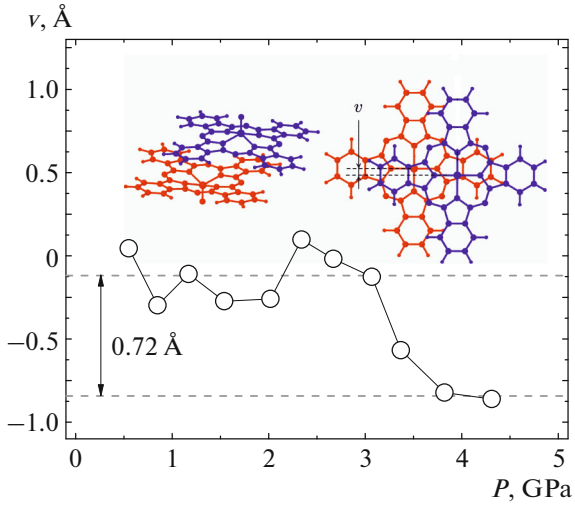

Fig. 6. (Color online) Baric dependences of the mutual vertical shift v of macrocycles in phthalocyanine molecules in the VOPc α phase. The vertical shift v exhibits a jumplike increase at $P > 3$ GPa.

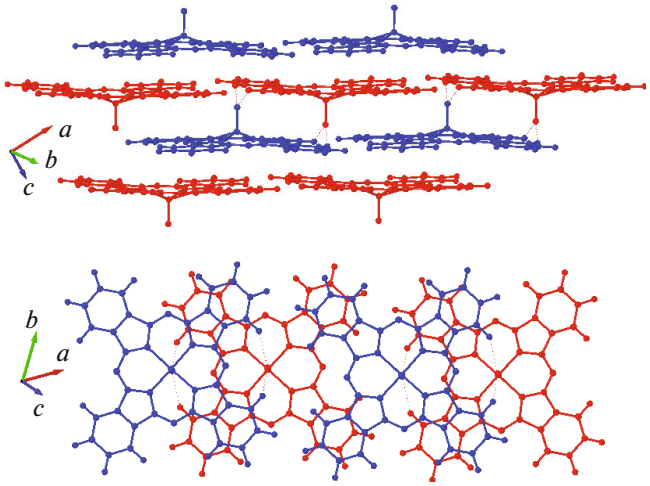

Fig. 7. (Color online) Network of short –CH···O contacts between one-dimensional phthalocyanine chains in the VOPc α phase.

induced feature in the 2.3–3.4 GPa interval of pressures, above which some phonon modes exhibit splitting and the baric shift coefficients of almost all modes tend to decrease. This behavior can be explained by densification of the network of intermolecular van der Waals contacts as a result of the contraction of crystalline lattice of the VOPc α phase. The baric dependence of the unit cell volume of the α phase measured up to 4 GPa is a smooth and monotonic function of pressure that is adequately described by the Murnaghan equation of state (1). Based on the obtained Raman spectroscopy and XRD data were used to determine the Grüneisen parameters of various phonon modes of VOPc.

FUNDING

This investigation was performed in accordance with the Program of State Orders to the Institute of Solid State Physics (Chernogolovka) and supported in part by the Russian Acad-

emy of Sciences the framework of the "Physics of Condensed State and Materials of New Generation" Program.

REFERENCES

1. D. Wöhrle, in *Phthalocyanines: Properties and Applications,* Ed. by C. C. Leznoff and A. B. P. Lever, Adv. Mater. 5, 942 (1993).
2. D. Hohnholz, S. Steinbrecher, and M. Hanack, J. Mol. Struct. **521**, 231 (2000).
3. J. Robertson, A. Smith, J. Duignan, et al., Appl. Phys. Lett. **78**, 1183 (2001).
4. J. Xue, S. Uchida, B. Rand, et al., Appl. Phys. Lett. **85**, 5757 (2004).
5. B. J. Palys, D. M. W. van der Ham, W. Briels, and D. Feil, J. Raman Spectrosc. **26**, 63 (1995).
6. D. R. Tackley, G. Dent, and W. E. Smith, Phys. Chem. Chem. Phys. **2**, 3949 (2000).
7. D. R. Tackley, G. Dent, and W. E. Smith, Phys. Chem. Chem. Phys. **3**, 1419 (2001).
8. S. Heutz, S. M. Baliss, R. L. Middleton, et al., J. Phys. Chem. B **104**, 7124 (2000).
9. S. Yim, S. Heutz, and T. S. Jones, J. Appl. Phys. **91**, 3632 (2002).
10. N. L. Levshin, S. G. Yudin, E. A. Krylova, and A. T. Zlatkin, Russ. J. Phys. Chem. A **82**, 1921 (2008).
11. J. Tobik and E. Tosatti, J. Phys. Chem. **111**, 12570 (2007).
12. D. V. Konarev, A. V. Kuzmin, M. A. Faraonov, et al., Chem.–Eur. J. **21**, 1014 (2015).
13. D. V. Konarev, M. A. Faraonov, A. V. Kuzmin, et al., New J. Chem. **41**, 6866 (2017).
14. D. V. Konarev, A. V. Kuzmin, S. S. Khasanov, et al., CrystEngComm. **20**, 385 (2018).
15. D. V. Konarev, A. V. Kuzmin, S. S. Khasanov, et al., Chem. - Asian J. **13**, 1552 (2018).
16. T. Inabe and H. Tajima, Chem. Rev. **104**, 5503 (2004).
17. D. E. C. Yu, M. Matsuda, H. Tajima, et al., J. Mater. Chem. **19**, 718 (2009).
18. J. Rimas Vaisnys and R. S. Kirk, Phys. Rev. **141**, 641 (1966).
19. A. Onodera, N. Kawai, and T. Kobayashi, Solid State Commun. **17**, 775 (1975).
20. A. V. Kuzmin, S. S. Khasanov, K. P. Meletov, and R. P. Shibaeva, J. Exp. Theor. Phys. **128**, 878 (2019).
21. A. Jayaraman, Rev. Sci. Instrum. **57**, 1013 (1986).
22. Rigaku Oxford Diffraction, *CrysAlisProSoftware System, Version 1.171.39.46* (Rigaku Corp., Oxford, UK, 2018).
23. N. Döbelin and R. Kleeberg, J. Appl. Crystallogr. **48**, 1573 (2015).
24. C. H. Griffiths, M. S. Walker, and P. Goldstein, Mol. Cryst. Liq. Cryst. **33**, 149 (1976).
25. R. F. Ziolo, C. H. Griffiths, and J. M. Troup, J. Chem. Soc., Dalton Trans. **11**, 2300 (1980).
26. W. Hiller, J. Strahle, W. Kobel, and M. Z. Hanack, Kristallogr. **159**, 173 (1982).
27. K. P. Meletov, Phys. Solid State **55**, 581 (2013).
28. S. N. Vaidya and G. C. Kennedy, J. Chem. Phys. **55**, 987 (1971).
29. T. V. Basova, V. G. Kiselev, B.-E. Schuster, et al., J. Raman Spectrosc. **40**, 2080 (2009).

Translated by P. Pozdeev